



**HAL**  
open science

## Helical defects in smectic- A and smectic- A\* phases

Claire Meyer, Yuriy Nastishin, Maurice Kleman

► **To cite this version:**

Claire Meyer, Yuriy Nastishin, Maurice Kleman. Helical defects in smectic- A and smectic- A\* phases. Physical Review E , 2010, 82, 10.1103/PhysRevE.82.031704 . insu-03605286

**HAL Id: insu-03605286**

**<https://insu.hal.science/insu-03605286>**

Submitted on 11 Mar 2022

**HAL** is a multi-disciplinary open access archive for the deposit and dissemination of scientific research documents, whether they are published or not. The documents may come from teaching and research institutions in France or abroad, or from public or private research centers.

L'archive ouverte pluridisciplinaire **HAL**, est destinée au dépôt et à la diffusion de documents scientifiques de niveau recherche, publiés ou non, émanant des établissements d'enseignement et de recherche français ou étrangers, des laboratoires publics ou privés.



Distributed under a Creative Commons Attribution 4.0 International License

**Helical defects in smectic-A and smectic-A\* phases**

Claire Meyer\*

*Laboratoire de Physique des Systèmes Complexes, Université de Picardie Jules Verne, 33 rue Saint-Leu, 80039 Amiens, France*

Yuriy Nastishin†

*Institute of Physical Optics, 23 Dragomanov Str., Lviv 79005, Ukraine*

Maurice Kleman‡

*Institut de Physique du Globe de Paris (UMR CNRS 7154), 1 rue Jussieu, 75238 Paris Cédex 05, France*

(Received 29 April 2010; published 21 September 2010)

There are two categories of helical line defects in Sm-A phases: screw dislocations of small Burgers vectors and double helices (DHs), whose macroscopic configuration constitutes a mode of splitting of screw dislocations of giant Burgers vectors. Their counterparts in Sm-A\*s (Sm-A\*s with chiral molecules) show a number of differences with the former and are investigated theoretically on the basis of recent observations [C. Meyer *et al.*, *Liq. Cryst.* **37**, 1047 (2010)]. The first part of the paper is a short review of the main features of helical defects in Sm-A's proper. In Sm-A\*s, small Burgers vector screw dislocations with the same chirality as the high-temperature  $N^*$  phase are favored over the opposite ones, a result that is related to the defect core singularity. This is also true for the macroscopic DH\*s for a more subtle reason; we advance that the DH\* nucleation at the  $N^* \rightarrow \text{Sm-A}^*$  transition stems from a peculiar texture of the cybotactic groups, akin in the ideal case to a set of two twisted  $\chi$  disclinations in the  $N^*$  phase, linked by a stacking fault of continuous disclinations. This stacking fault vanishes in the Sm-A\* phase, and one recovers a DH\* much similar to a DH but with the appropriate chirality. Cases that differ from ideality are described: they involve small Burgers vector screw dislocations and can be evoked to explain the numerous observed distorted double helices (the Darboux condition is not obeyed) and twisted ribbons. The case when the  $N^* \rightarrow \text{Sm-A}^*$  transition is type II (presence of a twist grain boundary phase in between) is briefly discussed.

DOI: [10.1103/PhysRevE.82.031704](https://doi.org/10.1103/PhysRevE.82.031704)

PACS number(s): 61.30.Jf, 64.70.M–

**I. INTRODUCTION**

Disclination double helices (DHs) were first observed by Williams [2] in the smectic-A (Sm-A) phase of cyano benzilidene octyl oxyanilin (CBOOA) and readily interpreted as screw dislocations with a giant Burgers vector, in the frame of a model which also inspired the interpretation of several other observations (in the B7 phase of bent-core liquid crystals, in some chromosomes, etc.) later recalled in this paper. Some textures recently observed in smectic-A phases of chiral molecules (Sm-A\*), which look at first sight of a much similar nature as DHs in Sm-A's [1]—which we shall denote by DH\*—but in fact exhibit striking differences, have led us to set the question of the screw dislocations with a giant Burgers vector from another point of view; isometric deformations, chirality, focal conic domains (FCDs), and screw dislocation modalities precisely when the Burgers vector is giant, according to whether the sample is chiral or not, are the key topics of this investigation.

We call *isometric defects* [3] the defects that preserve the layer parallelism, thereby their equidistance in some domain (generically of a finite size). Ideal FCDs are macroscopic domains of that type. A FCD involves a considerable number of layers related to two singular lines, namely, *two cofocal*

*conics*, an ellipse, and a hyperbola (in special cases degenerated into a circle and a straight line). The molecules extend along straight segments joining any pair of points, one of the ellipses, and the other on the hyperbola. The domain thus geometrically related to the two conics is made of *equidistant* layers; the compression energy is minimized at the expense of curvature energy. The total energy is rather small; the layers take in this domain the shape of Dupin cyclides, generally limited to a portion of negative Gaussian curvature, such that the domain is of finite extent; cf. [4] and references therein. We shall loosely call such a domain a *macroscopic defect*, although the singularities of the domain are line defects whose core size is generically microscopic.

*Macroscopic Sm-A* defects are not always ideally isometric; one finds the following:

(1) Local imperfections along the conics, called *kinks*, to which dislocations are attached. These kinks can be microscopic objects, but they often gather along macroscopic imperfections, to which a large density of dislocations is attached, or a dislocation with a unique giant Burgers vector [5]. On the whole, one still observes FCDs, but with pairs of singular lines that are conics with analyzable irregularities,

(2) Apart from ideal and imperfect FCDs, more global distortions that can be described as a family of portions of FCDs attached along incomplete conics, as pointed out in [2]. This results in a unique pair of linear singularities, which are intertwined and thus take the shape of a *double helix*, right or left twisted according to the case. Similarly to the FCDs they appear as a response to the deformation of smec-

\*claire.meyer@u-picardie.fr

†ynastish@kent.edu

‡maurice.kleman@mines.org

tic layers under the requirement of isometry, although isometry is eventually not fully satisfied.

The topic of FCDs and of their kinks is fairly well covered in the literature (see [4] for a recent review). A part of this paper is devoted to a detailed description of DHs. We shall argue that they constitute a modality of screw dislocations with giant Burgers vectors.

DHs are the only *helical defects* that are currently visible in Sm-A's with *achiral molecules*. Their *ideal* characteristics and their occurrences in observations are reviewed in Secs. III and IV. There are more modalities of screw dislocations with large Burgers vectors in smectics with *chiral molecules* (Sm-A\*'s). The rest of this paper explores results about these classes of helical defects, in particular: (a) which factors determine the sign of the twist and (b) how the DH\* structure differs from the DH, and how it is related to the molecular configuration.

We refer the reader to [1] for detailed observations of all these helical defects and their modes of disappearance when approaching the high-temperature transition, in the compounds of cholesteryl nonanoate (C9, also called cholesteryl pelargonate) and cholesteryl tetradecanoate (C14, also called cholesteryl myristate).<sup>1</sup>

Section II is a quick review of the elastic properties of Sm-A's (and Sm-A\*'s), in which we stress the isometric properties of FCDs. Except if specifically stated, the notation DH will refer to the common properties of DH and DH\*; the notion of ideal DH applies to a DH\*.

## II. ELASTIC PROPERTIES AT A MACROSCOPIC SCALE: ISOMETRY

As a rule, the geometry of macroscopic smectic defects results from the trend toward isometry, in contrast to defects like dislocations of small Burgers vectors, whose (meta)stability results from a competition between two contributions—*strain* elasticity, i.e., the compressibility of the layers, and *curvature* elasticity, i.e., the curvature of the layers—that have different ranges of action. Let indeed  $R$  be the typical size of a domain affected by the presence of some defect, submitted to some compression or tension: the strain energy scales as  $F_{strain} = \int f_{strain} \approx BR^3$ , and the curvature energy scales as  $F_{curv} = \int f_{curv} \approx K_1 R$ .  $B$  and  $K_1$  are the classical moduli of the free-energy density

$$f = \frac{1}{2}K_1(\text{div } \mathbf{n})^2 + \frac{1}{2}B\left(1 - \frac{d}{d_0}\right)^2 + \bar{K}\sigma_1\sigma_2 + \frac{1}{2}K_2(q + \mathbf{n} \cdot \text{curl } \mathbf{n})^2, \quad (1)$$

where  $\mathbf{n}(x,y,z)$  is the director,  $d_0$  is the thickness of the undeformed layer,  $d(x,y,z) > 0$  is the thickness of the deformed layer, and  $\sigma_1, \sigma_2$  are the radii of curvatures of the layer at the point  $x,y,z$ . The term  $\bar{K}\sigma_1\sigma_2$  is integrable to a

surface term and should be considered whenever the topology of layers is altered (e.g., FCDs and DHs, which cannot transform smoothly one into the other). When comparing different geometric realizations having the same topology (determined by the nature of the defects), we can forget the role of this term. A twist term  $f_{twist} = 1/2K_2(q + \mathbf{n} \cdot \text{curl } \mathbf{n})^2$  has been introduced on purpose, where  $q$  measures the molecular chirality. The relation

$$\mathbf{n} \cdot \text{curl } \mathbf{n} = 0 \quad (2)$$

is a necessary and sufficient condition for a vector field  $\mathbf{n}$  to be orthogonal to a set of surfaces; thereby, this relation is obeyed in a smectic phase, except possibly where the order parameter is broken, i.e., at a singularity. Thus, generically, we have not to take the  $f_{twist}$  term into account.

The ratio  $F_{strain}/F_{curv} = (R/\lambda_1)^2$ ,  $\lambda_1^2 = K_1/B$  is much larger than unity as soon as  $R > \lambda_1$ .<sup>2</sup> Therefore, the dominant distortion visible at a macroscopic scale should be a curvature with vanishing strain: the layers are parallel, i.e., macroscopic defects are likely to be isometric, at least in some limited domain; the singularities are the *focal sheets* (the locus of the centers of curvature) of the parallel layers. On the other hand, at small scales, the strain energy and the curvature energy can balance. A FCD is a macroscopic defect; it is the only perfectly isometric solution with focal surfaces degenerated to *line* defects. Because of the finiteness of the domain, nonisometric deformations necessarily occur in the vicinity of FCDs. The embedding of FCDs is another problem, not discussed here (see [4]). Let us just retain that one can find textures where the director field varies continuously at the contact between the FCD and the Sm-A matrix.

## III. DH DOMAINS

Their construction is as follows. In a first step consider a *ruled helicoid*, i.e., a surface generated by a straight line  $\Delta$  rotating helically with an invariable pitch  $p$  along a straight axis  $\Lambda$ . This is a minimal surface:  $\text{div } \mathbf{n} = \pm(\sigma_1 + \sigma_2) = 0$ , where  $\mathbf{n}$  is the unit normal to the helicoid. At a distance from the axis large compared to  $|p|$ , the successive layer turns of the helicoid are practically parallel, with a repeat distance measured along the axis equal to  $|p|$ . This is precisely the geometry expected for a screw dislocation of Burgers vector  $|b| = |p| = 2d_0$ .<sup>3</sup> The energy is small: the curvature energy vanishes since the layer takes the shape of a minimal surface, and the strain energy density is of a small order (it scales as  $r^{-4}$ , where  $r$  is the radial distance to the axis); see Figs. 26(a) and 26(b) and a discussion in [6]. Ruled-helical layers in a Sm-A are the more favored as  $\bar{K}$  is more positive since in a helicoid  $\sigma_1\sigma_2 < 0$  [Eq. (1)].

<sup>2</sup> $\lambda_1$  is a material length which cannot be much different from  $d_0$ , the thickness of an unperturbed layer.

<sup>3</sup>The factor of 2 stems from the fact that  $\Delta$  here is an infinite straight line, as in Fig. 1;  $p$  is a *unit* Burgers vector if  $\Delta$  is restricted to half a straight line limited to the axis  $\Lambda$ . This point is discussed in Sec. VI A.

<sup>1</sup>Of course C9 and C14 both have a  $N^*$  phase above the Sm-A\* phase; C9 exhibits a TGBA phase between Sm-A\* and  $N^*$ , in a small range of temperature (cf. [1], and references therein).

Assume that the pitch is giant:  $|p| \gg d_0$ . Then, by piling up a family of helicoids on the central ruled helicoid, parallel to it, with a repeat distance  $d_0$ , all with pitch  $|p|$ , one gets a dislocation with a giant Burgers vector  $b=p=2nd_0$ ,  $n \in \mathbb{Z}$ .<sup>4</sup>

Such a stacking of *parallel* layers brings a new feature. These parallel layers have two *focal sheets* along which the layers have an infinite curvature. The singularity is surface-like, not linelike as for FCDs; furthermore, these focal sheets intersect an infinite number of times. Whereas this construction yields a very small energy of curvature in the region devoid of the presence of the focal sheets (since it vanishes on the central layer), it would yield a considerable energy in the region where the sheets appear. The region devoid of focal sheets is the interior of a cylinder  $C$  of radius  $|p|/2\pi$  centered on the axis of the helicoids, on which cylinder the two focal sheets abut along two helices of pitch  $|p|$ , with the same chirality as the helicoids, shifted one with respect to the other by a distance  $|p|/2$  along the axis, constituting the cuspidal lines of the two focal surfaces of the helical set. The layers about the two helices are deployed along two  $k=1/2$  disclinations (see Fig. 1). This geometry results rigorously from the parallel stacking on a ruled helicoid; however, because the region outside cannot be of the kind suggested by the focal sheet configuration—the focal *surfaces* vanish, just remain their cuspidal lines, the two helices—and the configuration along  $C$  is perturbed, the observed configurations of the double helices are much distorted compared to the ideal DH. Here are some examples.

#### IV. SOME PHYSICAL REALIZATIONS OF DOUBLE HELICAL GEOMETRIES

It is in the B7 phase, made of bent-core molecules [3], that we find the best empirical realization of an ideal arrangement of a double helical singularity with perfectly parallel smectic layers *inside*  $C$ . The dominant mode of stability of these layers, parallelism and helicity,<sup>5</sup> is perfectly satisfied inside, as illustrated Fig. 1. The layers are completely destroyed *outside*  $C$ , where the B7 order parameter is broken to an isotropic phase.

The ideal construction inside  $C$  is a commonplace template not only for very different systems such as the B7 phase and Sm-A's, but also for biological objects among which the chromosomes of dinoflagellate [7]. On the other hand, the DHs that are observed in smectics, while forming a configuration topologically equivalent to this model, suffer considerable distortions that bring them far from the ideal helical ribbons. Outside  $C$ , the layer stacking is quasi-isometric, with an orientation globally orthogonal to the axis of the double helix (see Fig. 2).

<sup>4</sup>We give the same sign to the Burgers vector and to the pitch of the dislocation layers (the convention of sign is discussed in Appendix A).

<sup>5</sup>The helicity we are alluding to relates to the inner structure of the layers, which can be figured out, geometrically, as a set of parallel columns. These columns suffer a twist from one layer to the next. The helical texture is compatible altogether with the requirement of parallelism of the layers and chirality of the intralayer columns; see [3] for a detailed account.

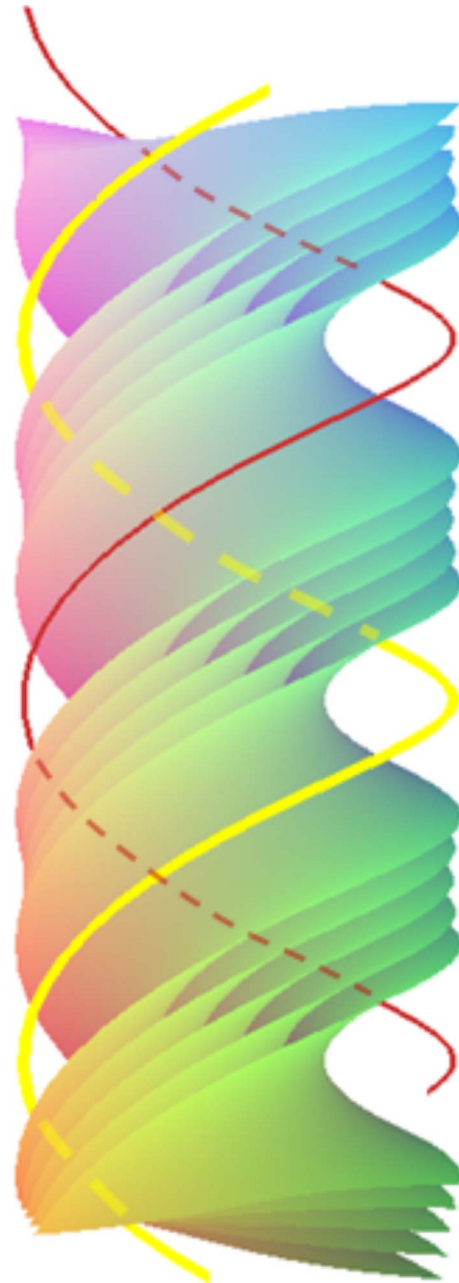


FIG. 1. (Color online) Parallel helicoidal surfaces inside  $C$  and their two cuspidal lines modeling an arrangement of smectic layers with two helical disclinations, for a giant Burgers vector dislocation in its split mode;  $p=2nd_0$ . For clarity one of the disclinations (yellow/light gray) is shown thicker than the other one (red/gray dark).

In the CBOOA Sm-A phase of Ref. [2], the sample is confined between two slides with a planar alignment, and the helical axis is parallel to the slides. This obtains by cooling the sample from its nematic state to the smectic state; as a result any half-integer disclination line  $k=1/2$  parallel to the slides is the source of a set of double helical lines, whose disclination nature is thereby corroborated by this origin.

Figure 3 shows how DHs appear in an 8CB compound. The DH nucleates from a single helix that is the Sm-A trans-

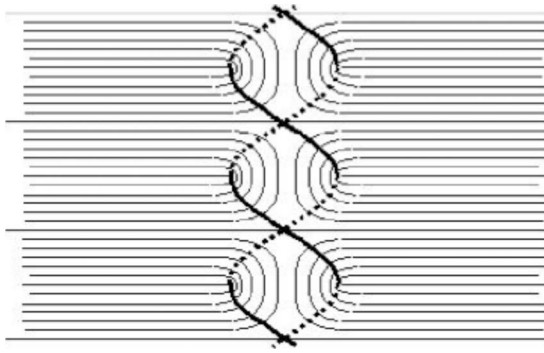


FIG. 2. Sketch of the smectic layers (thin lines) inside and outside  $C$  and double helical disclinations (thick lines) in a DH. In reality, the double helix is much distorted in a Sm-A, but the topology is the same. Isometry is globally preserved, as explained in Sec. V.

formation of the  $k=1/2$  line in the nematic phase, orthogonally to this twisted line.

It is easy to observe DHs in other nematogenic materials such as 8CB and 9CB, as well as in the Sm-A phase of chiral materials exhibiting a  $N^*$ -Sm- $A^*$  transition, but they are much different from DHs in Sm- $A$ 's. Smectic phases in chiral materials and achiral materials are not structurally equivalent. It has been recommended [9] to distinguish the smectic- $A$  phase in chiral materials—denoting it with a star (Sm- $A^*$ )—from the nonchiral phase (Sm- $A$ ). The point group of a nonchiral Sm- $A$  is  $\infty/m$  (or  $D_{\infty h}$  in other notation), whereas the symmetry group of the Sm- $A^*$  in chiral materials is  $\infty \cdot 2$  (or  $D_{\infty}$ ). The difference in the symmetry implies a difference in some physical properties. The electroclinic effect, possible in a Sm- $A^*$  and forbidden in a Sm- $A$ , is an example [10]. The nature of helical macroscopic defects is another one.

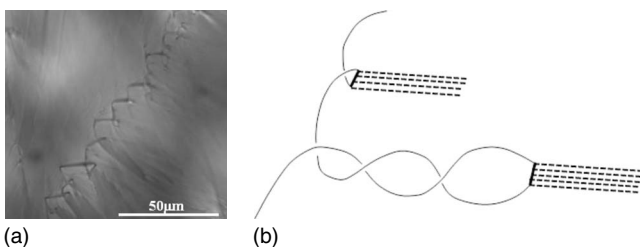


FIG. 3. (a)  $k=1/2$  wedge disclination line in the Sm- $A$  phase of 8CB, with the shape of a single helix. This disclination arises from a wedge line in the  $N$  phase. The mean director orientations in the regions above and below the helix are the same as the orientations in the  $N$  phase. The DHs nucleate orthogonally to the disclination line, to which clusters of screw dislocations are attached—orthogonal to the layers, visible at the bottom right of the picture. This attachment demonstrates the screw character of the nucleating DHs; (b) illustration of the nucleation and growth of a DH in a direction orthogonal to the wedge disclination (adapted from Kleman [8], Chap. 5). The dashed lines figure out the attached screw dislocations. This mechanism, which has been observed by Williams [2], is not visible on the photograph in (a).

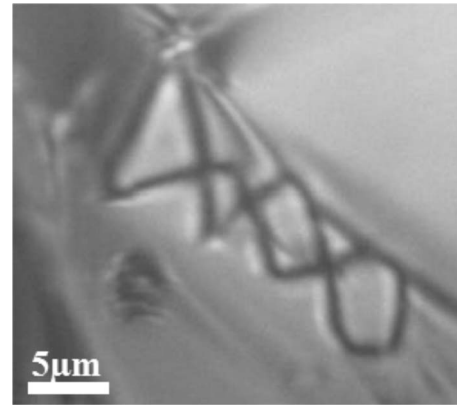


FIG. 4. Darboux's condition obeyed for a DH in Sm- $A$  of 8CB.

### V. DHs AND FCDs, COMPARED: THE DARBOUX CONDITION

Ideal FCDs, in Sm- $A$ 's and Sm- $A^*$ 's, exhibit a remarkable feature, namely, that the projections of the cofocal conics intersect at right angles. This is a consequence of the following theorem ([11], Sec. IV, Chap. 12): consider a congruence of straight lines orthogonal to a set of parallel surfaces; in short, with a congruence of normals, and any one of these normals, say  $S$ , the two planes  $P_1$  and  $P_2$  tangent to the focal sheets at the points of contact  $M_1$  and  $M_2$  of  $S$  cross at right angles. For an observer who looks in the direction of  $S$ , the focal sheets seem to be orthogonal (call this *the Darboux condition*, in brief DC). If the focal sheets are degenerated to lines, as in FCDs—whose integral lines of the director field form such a congruence of normals—these lines look orthogonal in projection along any line of sight, i.e., any line joining any point on the ellipse to any point on the hyperbola. Reciprocally, if this optical property is satisfied, one expects that the lines of sight belong to a congruence of normals.

DC is also satisfied for ideal DHs in Sm- $A$ 's, in which DHs are made of a congruence of normals to a central ruled helicoid. However, empirically, only the cuspidal edges of the focal sheets are visible, and the only normals of the congruence that intersect the two helices are along diameters of the cylinder centered on the DH axis, intersecting this axis at right angles. These are the only lines of sight empirically useful, so that DC is observed, rather approximately, when the DH is in the plane of the sample, i.e., approximately perpendicular to the axis of the microscope (see Fig. 4), when the lines of sight are practically orthogonal to the DH axis.

The tangents to the two helical cusp lines traced on the focal sheets—the DH disclination lines—at the points of contact  $M_1$  and  $M_2$  of  $S$ , belong together with  $S$  to the planes  $P_1$  and  $P_2$  tangent to these focal sheets. Most surprisingly, DC is still satisfied (with practically the same degree of uncertainty—or of perfection—one can observe in the practically ideal case of the DHs in the B7 phase) even when the DH is much distorted about the average helical axis, as it is the case in all the Sm- $A$  samples that have been observed.

This tells in favor of the existence of a congruence of normals, thereby of parallel layers, and of the *persisting validity of the condition of isometry, notwithstanding the distortion of the double helix*. Let us now recall that *screw dislocations* do not modify much the parallelism of the layers they cross. One can infer from this remark that the large-scale distortion of the DH in Sm-A's is controlled by sets of screw dislocation segments orthogonal to the layers inside the domain bounded by the helical strands; these dislocations have to emerge outside this domain due to the conservation of the Burgers vector or to terminate on kinks on the helical disclinations. They contribute to the relaxation of the elastic deformation due to the misfit between the layers inside and the layers outside.

While DC is practically the rule in Sm-A's, it is far from being obeyed in Sm-A\*'s. We therefore conclude that the layers are not parallel in the domain interested by the singularities: isometry is not satisfied in DH\*s. The associated stresses can be relaxed by *edge dislocations* (see [8], Chap. 6). This is in strong contrast with screw dislocations (of microscopic Burgers vector) which, as stated above, do not relax imperfections of parallelism.

## VI. SCREW DISLOCATIONS IN Sm-A's AND Sm-A\*'s, COMPARED

The FCDs present in a Sm-A\* phase differ in no respect from those of achiral smectics; the molecular chirality plays no role in their (meta)stability. This is not so for textures that involve screw dislocations. Screw dislocations of opposite Burgers vectors are not equivalent in a Sm-A\* phase. We show this for small Burgers vectors, first, and then discuss of the consequences for large (giant) Burgers vectors.

### A. Screw dislocations of small Burgers vectors

The condition  $\mathbf{n} \cdot \text{curl } \mathbf{n} = 0$  is strictly obeyed in a layered medium; it constitutes a necessary and sufficient condition of integration of a vector field  $\mathbf{n}$ . In the presence of a screw dislocation that exhibits a core singularity this condition is changed to

$$\mathbf{n} \cdot \text{curl } \mathbf{n} = -b \delta(x) \delta(y), \quad (3)$$

where  $b$  is the Burgers vector in the  $\hat{z}$  direction, and the directions  $\hat{x}$  and  $\hat{y}$  are orthogonal directions in the plane orthogonal to the dislocation line (see Appendix A).

Consider the chiral term in the free-energy density

$$f_{\text{twist}} = \frac{1}{2} K_2 (q + \mathbf{n} \cdot \text{curl } \mathbf{n})^2. \quad (4)$$

Here,  $q = 2\pi/p$ , where  $p$  is a measure of the rotating power of the medium in the Sm-A\* phase. This term plays no role if  $\mathbf{n} \cdot \text{curl } \mathbf{n} \equiv 0$  since its presence then amounts to a constant shift of the free energy. But in the presence of a screw dislocation one has to take two terms into account. The first one  $\frac{1}{2} K_2 (\mathbf{n} \cdot \text{curl } \mathbf{n})^2$  does not depend on the sign of the Burgers vector and furthermore does not involve the presence or absence of chirality. The second one  $K_2 q \mathbf{n} \cdot \text{curl } \mathbf{n} = -K_2 q b \delta(x) \delta(y)$  vanishes identically in a Sm-A, but takes opposite values for dislocations of opposite Burgers vectors

in a Sm-A\*. When integrated over the plane  $\hat{x}\hat{y}$  it yields a chiral contribution per unit length of line to the core energy of the dislocation:

$$F_{c,\text{twist}} = -K_2 q b, \quad (5)$$

which depends on the sign of the Burgers vector: it is negative if the dislocation and the molecular chirality have the same sign. In the Sm-A\* phase, dislocations of opposite signs behave quite differently; *the screw dislocations of the same chirality as the molecular chirality are favored*.

For a dislocation of Burgers vector  $|b| = d_0$ , which is topologically equivalent to a half-ruled helicoid [[6], Fig. 26(a)], the core singularity, whose size  $r_c \approx d_0$ , has an energy  $F_c \approx \pi B d_0^2 + K_1 - K_2 q b$ . All together,

$$\begin{aligned} F_{b=\pm d_0} &\approx \frac{B b^4}{128 \pi^3 r_c^2} + \pi B b^2 + K_1 - K_2 q b \\ &\approx \frac{B d_0^2}{128 \pi^3} + \pi B d_0^2 + K_1 - K_2 q b. \end{aligned} \quad (6)$$

Based on Eq. (6), a very simplified model of the stability of the twist grain boundary (TGB) phase may go as follows (cf. also [12], Chap. 9). Compare  $F_{c,\text{twist}} = -K_2 q b$  and the rest of the core contributions—which we restrict to  $F_{c,\text{splay}} \approx K_1$ , justified since  $F_{c,\text{splay}} \approx F_{c,\text{strain}}$ . One gets  $|F_{c,\text{twist}}|/F_{c,\text{splay}} \approx (K_2/K_1)|q|d_0$ , with  $b = \pm d_0, bq > 0$ . The stability of the TGBA phase would then require

$$\alpha = 1 - |q|d_0 \frac{K_2}{K_1} < 0. \quad (7)$$

The condition  $\alpha < 0$ , which also reads

$$\varepsilon_2 = \frac{K_2}{K_1} |q|d_0 = \frac{\lambda_2^2}{\lambda_1^2} |q|d_0 > 1, \quad (8)$$

plays the role, in this simplified theory of the TGBA stability, of the more sophisticated Ginzburg-Landau condition  $\kappa_2 = \lambda_2/\xi > 2^{-1/2}$ , with  $\lambda_2$  being the twist penetration length and  $\xi$  the coherence length [13]. According to [14],  $q^{-1} \propto K_2 \sim (|T - T_c|/T_c)^{-\nu}$ ;  $\nu$  is the exponent of the coherence length. Thus  $\varepsilon_2$ , like  $\kappa_2$ , is little dependent on  $T$ .

For a dislocation of Burgers vector  $|b| = 2d_0$ , which has the topology of a complete ruled helicoid, the splay contribution  $F_{c,\text{splay}}$  is on the same order of magnitude as for  $F_{b=\pm d_0}$  above, and the main contribution to the line energy in the core is due to the strain,  $F_{c,\text{strain}} \approx 4\pi B d_0^2$ . All together,

$$\begin{aligned} F_{b=\pm 2d_0} &\approx \frac{B d_0^4}{8 \pi^3 r_c^2} + 4\pi B d_0^2 - K_2 q b \\ &\approx \frac{B d_0^2}{32 \pi^3} + 4\pi B d_0^2 + K_1 - K_2 q b, \end{aligned} \quad (9)$$

where the first term is the energy outside the core,  $r_c \approx 2d_0$ . The core contribution is prevailing.

Let us compare  $F_2 = F_{b=\pm 2d_0}$  and  $F_1 = F_{b=\pm d_0}$  when  $qb > 0$ , i.e., when the twist core energy is stabilizing. One gets

$$\frac{F_2 - F_1}{K_1} \approx 3\pi \frac{d_0^2}{\lambda_1^2} - \varepsilon_2.$$

Because of the large factor  $3\pi$ , the quantity  $F_2 - F_1$  is positive in most cases, except possibly when the TGBA phase is stable and  $\varepsilon_2$  is very large [cf. Eq. (8)]. We assume in the sequel that the  $b = \pm d_0$  dislocations have a smaller energy than the  $b = \pm 2d_0$  dislocations.

### B. Interplay of screw dislocations of small and large Burgers vectors

In a DH, the layers (the inner helicoids and their outer prolongations) are well defined even in the vicinity of the disclinations; thereby, the integrability condition  $\mathbf{n} \cdot \text{curl } \mathbf{n} = 0$  is satisfied everywhere: there is no contribution of the twist  $K_2$  to the energy. Within the frame of a simplified analysis of the energy of a DH, one assumes that the splay energy of the inner part is negligible since it is vanishing in the ideal case on the central layer. Therefore, as already noticed in [3], the main contribution to the splay energy comes from the two helical disclinations whose length is  $|b|\sqrt{2}$  per turn,  $L\sqrt{2}$  per length  $L$  measured along the axis of the DH.<sup>6</sup> We thus expect a bulk energy on the order of  $F_{DH,splay} \approx \pi\sqrt{2}K_1 \ln(n/4)$ ,  $n > 0$  per unit length of helical axis.<sup>7</sup> To this quantity has to be added a core energy, which we estimate as usual as  $F_{DH,c} \approx \sqrt{2}K_1$ . Now, the contact between the inner ideal configuration and the outer configuration of parallel layers at a distance cannot be in perfect register, so that one expects a source of strain energy on a cylinder of radius  $R = |b|/2\pi$ , in a region of thickness  $d_0$ ; hence,  $F_{DH,strain} \approx B(2\pi R d_0) = nBd_0^2$ . A part of this energy is relaxed by the distortion of the DH, as claimed above. However,  $F_{DH,strain}$  gives a plausible dependence on  $n$  of this strain contribution, so that we keep this expression for the sake of simplicity. Therefore, the total line energy can be written as

$$F_{DH} \approx \sqrt{2}K_1\pi \ln\left(\frac{en}{4}\right) + nBd_0^2. \quad (10)$$

Achiral case  $q=0$ : Comparing  $F_{DH}$  to  $F_{|b|=d_0}$ , a DH of Burgers vector  $\pm nd_0$  is favored over a bundle of  $n$  unit dislocations  $b = \pm d_0$  for  $nBd_0^2 < Bn^4d_0^2/(128\pi^2r_c^2)$ , i.e., for  $n^3 \gtrsim 128\pi^3$ ,  $\rightarrow n > 16$ .

Chiral case  $q \neq 0$ : In order to compare the expression in Eq. (10) to that one of a favored dislocation  $F_{|b|=d_0}$ ,  $bq > 0$ , we consider the quantity

$$\begin{aligned} \Delta F &= F_{DH} - nF_{|b|=d_0} \\ &\approx K_1 \left[ \pi\sqrt{2} \ln\left(\frac{en}{4}\right) - n \left( 1 - \frac{d_0^2}{\lambda_1^2} - |q|d_0 \frac{K_2}{K_1} \right) \right] \\ &= K_1 \left[ \pi\sqrt{2} \ln\left(\frac{en}{4}\right) - n\alpha + n \frac{d_0^2}{\lambda_1^2} \right]. \end{aligned} \quad (11)$$

<sup>6</sup>The dependence in  $b$  has disappeared.

<sup>7</sup>Figure 4 appearing in the logarithm relates to the number of layers that are involved about a disclination: it is  $|b|/2d_0 = n/2$  (see Fig. 2, where  $n=12$ ). There are two disclinations, hence the nonappearance of the usual factor of 1/2 in this expression.

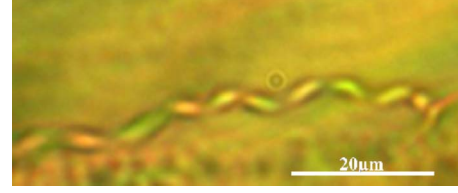


FIG. 5. (Color online) DH\* in a C14 sample; the Darboux condition is not obeyed.

The logarithmic term can be neglected in Eq. (11). Then two opposite situations might occur in the Sm-A\* phase:

$\alpha > d_0^2/\lambda_1^2 \rightarrow \Delta F < 0$ : DH\*s are preferred over bundles of unit Burgers vector dislocations. Since  $\alpha > 0$ , the transition is type I ( $N^* \rightarrow \text{Sm-A}^*$ , the analog of a transition from a normal metal to a superconductor).

$\alpha < d_0^2/\lambda_1^2 \rightarrow \Delta F > 0$ : the transition is either type I when  $\alpha > 0$  or type II ( $N^* \rightarrow \text{TGBA} \rightarrow \text{Sm-A}^*$ ) when  $\alpha < 0$ . Then the DH\*s tolerate numerous imperfections, in particular bundles of unit screw dislocations of the appropriate sign.

### C. General comments on DH\*s

This classification in function of  $\alpha$  suggests that there are *three* types of relationships between macroscopic helical defects and microscopic screw dislocations, depending on whether (i)  $\alpha < 0$ , (ii)  $0 < \alpha < d_0^2/\lambda_1^2$ , or (iii)  $\alpha > d_0^2/\lambda_1^2$ . Only the first case is of type II. It obeys the condition  $\Delta F > 0$ , which is also true for case (ii). Thus, one expects very similar microdefect-macrodefect interactions for type II specimens and type I [case (ii)]. We shall loosely speak of *type I helical defects*—or type I DH\*s—in case (iii) and *type II helical defects*—or type II DH\*s—in case (i).

In Sec. VII we argue that the differences between type I DH\*s and type II DH\*s are (1) the frequent occurrence in type II DH\*s of *ribbons* stretched between the helical singularities (the notion of “inner cylinder” used previously in our description of DHs is no longer valid) and (2) the presence of striations transverse to these ribbons, which we attribute to the gathering in bundles of unit screw dislocations originating from the TGBs and linking the two DH\* disclinations (see Fig. 9 below). In type I,  $0 < \alpha < d_0^2/\lambda_1^2$  case, the screw dislocations should stem from the condensation of the twist of the director in the  $N^*$  phase in the form of screw dislocations.

Differences between DH\*s and DHs are easy to assess. A DH ideal geometry is compatible with the topology of a Sm-A\* phase, but it is not what is observed. The most conspicuous differences are the following:

DC is mostly generally not obeyed in DH\*s (see Figs. 5 and 6)—the usually well obeyed Kirchhoff’s relations at the nodes ( $\sum_i b_i = 0$ , easily checked because each  $b_i$  is proportional to the width of an ideal DH) where several DHs merge are not satisfied at all (both types of discrepancies can be explained by the distance between the helical singularities not being ideal and the layer packing being not isometric. These possibilities easily follow from the analysis (Sec. VII)—ribbons are visible all over the samples that have been studied.

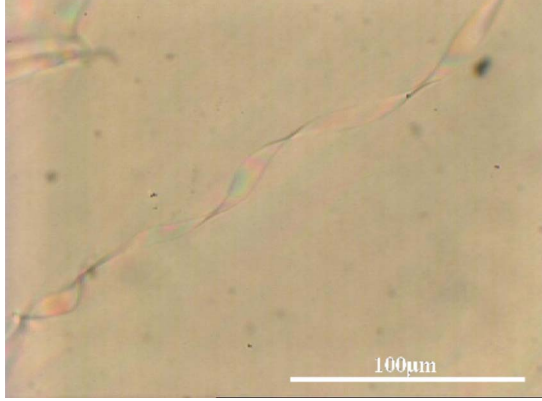


FIG. 6. (Color online)  $DH^*$  in a C9 sample; the Darboux condition is not obeyed.

We shall argue that all aspects peculiar to the helical defects in chiral phases are related to their generation, being remnants of the geometry of cybotactic groups in the  $N^*$  phase. On the other hand, we have yet no direct observations that clearly identify differences between the three  $DH^*$  cases. Therefore, our presentation will be partly speculative. Of course, the  $DH^*$ s, in their vast majority, appear to have the same chirality as the high-temperature  $N^*$  phase—this is a direct consequence of the foregoing developments.

## VII. NUCLEATION OF HELICAL DEFECTS IN A $Sm-A^*$ PHASE

We propose a geometric model of the precursory formation in the  $N^*$  phase of  $Sm-A^*$  helical defects.

### A. Cybotactic textures of the $N^*$ phase

A perfectly aligned  $N^*$  phase can be partitioned into a family of ruled helicoids as follows: let  $\Delta(0)$  denote some straight line orthogonal to the molecules in a cholesteric plane  $P(0)$  at  $z=0$ . Rotate  $\Delta(0)$  helically about the cholesteric axis at some point  $A \in \Delta(0)$ , with a pitch  $p$  equal to the cholesteric pitch. This results in a ruled helicoid  $\mathcal{H}(A)$  whose straight generators  $\Delta(z)$  are, everywhere in the  $N^*$  phase, orthogonal to the molecules of the cholesteric plane  $P(z)$  into which  $\Delta(0)$  has been transported by the helical translation. Take now a straight line  $\ell$  in  $P(0)$ , orthogonal to  $\Delta(0)$  at  $A$ , and associate to any point  $A_i \in \ell$  a helicoid  $\mathcal{H}(A_i)$  constructed in the same way as  $\mathcal{H}(A)$ , with generator in  $P(0)$  being a line  $\Delta_i(0)$  parallel to  $\Delta(0)$ . One gets a family of nonintersecting congruent ruled helicoids, which are dense in some domain of the  $N^*$  phase defined by the extension of  $\ell$ .

Conjecture: This partitioning provides a model for the transition from  $N^*$  to  $Sm-A^*$ . Consider a family of  $\mathcal{H}(A_i)$ 's made of ruled helicoids at distances  $d_0$  apart along  $\ell$ , belonging to a domain  $\mathcal{D}$  soon to be defined; as the temperature is decreased, these helicoids smoothly transform to smectic layers, to which the director field smoothly becomes orthogonal. We conjecture that this is the topology of a *cybotactic group* in  $N^*$  [12], turning to a  $Sm-A^*$  phase domain with helical layers at the transition. Since ruled helicoids are

minimal surfaces, their curvature energy is extremely small. Surely, they are not planar and do not reproduce the  $Sm-A^*$  ground state; their *helical torsion* has inherited the *twist*  $q = 2\pi/p$  of the  $N^*$  phase, but *stricto sensu* they are not twisted (the condition  $\mathbf{n} \cdot \text{curl } \mathbf{n} = 0$  is now satisfied).

Size of  $\mathcal{D}$ : The equation of  $\mathcal{H}$  for a point  $A$  chosen without loss of generality at the origin of the coordinates can be written as

$$\mathcal{H} \equiv \{r \cos \theta, r \sin \theta, \varpi \theta\}, \quad \theta \in \mathbb{R}, \quad r \in \mathbb{R}^+, \quad (12)$$

where  $\varpi = p/2\pi = q^{-1}$ ; the normal  $\boldsymbol{\nu}$  to  $\mathcal{H}$  at a point  $M$  with coordinates  $r, \theta, z(\theta = qz)$  and the tangent  $\boldsymbol{\tau}_r$  to the helix  $H(r)$  at  $r = \text{const}$  on the helicoid  $\mathcal{H}$  can be written as

$$\boldsymbol{\nu} = \frac{1}{N} \{-\varpi \sin qz, \varpi \cos qz, -r\}, \quad (13)$$

$$\boldsymbol{\tau}_r = \frac{1}{N} \{-r \sin qz, r \cos qz, \varpi\},$$

where  $N^2 = \varpi^2 + r^2$ ,  $\boldsymbol{\nu} \cdot \boldsymbol{\tau}_r = 0$ . The director in the cholesteric plane  $z$  is  $\mathbf{n} = \{-\sin qz, \cos qz, 0\}$ ; the angles  $\phi$  and  $\psi$  of  $\mathbf{n}$  with  $\boldsymbol{\nu}$  and  $\boldsymbol{\tau}_r$  are

$$\cos \phi = \boldsymbol{\nu} \cdot \mathbf{n} = \frac{\varpi}{N}, \quad \cos \psi = \boldsymbol{\tau}_r \cdot \mathbf{n} = \frac{r}{N} (= \sin \phi). \quad (14)$$

Here,  $\phi$  tends to  $\pi/2$  when  $qr$  is large, and is thus unacceptable in a  $Sm-A^*$  phase—this would yield a director  $\mathbf{n}$  parallel to the supposed layer—but has a small value when  $qr < 1$ ,  $\phi \approx qr$ . Hence, the acceptable domain  $\mathcal{D}$  is the inner part of a cylinder of radius  $r_{\mathcal{D}} \approx \varpi$ ; in  $\mathcal{D}$  the director  $\mathbf{n}$  of the cholesteric phase is almost orthogonal to  $\mathcal{H}$ , and  $\varpi$  appears as the coherence length at the  $N^* \rightarrow Sm-A^*$  transition. Thus, one expects that by small, smooth, and cooperative modifications of (a) the direction of  $\mathbf{n}$  ( $\mathbf{n}$  rotating toward the directions of the normals  $\boldsymbol{\nu}$  of the helical “layers”  $\mathcal{H}$ , i.e.,  $\phi \rightarrow 0$ ) and (b) the shape of the  $\mathcal{H}(A_i)$ 's, the family of ruled helicoids is transformed to a family of layers orthogonal to the director field, thereby exhibiting a smectic order parameter. The pitch  $p$  of the  $N^*$  phase diverges near the transition; thus, the size of  $\mathcal{D}$ ,  $r_{\mathcal{D}} = p/2\pi$ , depends on the kinetics of the transition and can in principle be quite large if the  $N^*$  phase is perfect on a large scale and the temperature decreases slowly.

The screw dislocation ideal texture of a cybotactic group in the  $N^*$  phase: One can expect that as a result of the cooperative deformation just described, the layers  $\mathcal{H}(\lambda)$  tend to become parallel—they are thereby no longer ruled, except possibly  $\mathcal{H}(0)$ —where  $\lambda$  denotes the signed distance to this central helicoid. Eventually, by a focalization of their normals, the parallel layers yield two disclinations of strength  $k=1/2$ , located at a distance  $b/2\pi \approx r_{\mathcal{D}}$  at the boundary of  $\mathcal{D}$ . Thus, in an ideal case, the cybotactic group  $\mathcal{D}$  takes at the  $N^* \rightarrow Sm-A^*$  transition the geometry of a screw dislocation of Burgers vector  $b=p$ , i.e., a  $DH^*$  domain.

But as long as the director field  $\mathbf{n}$  is not orthogonal to a family of layers (i.e., as long as the condition  $\mathbf{n} \cdot \text{curl } \mathbf{n} = 0$  is not fulfilled), the cybotactic group should better be considered as a deformed cholesteric: the director  $\mathbf{n}$  is almost orthogonal to the helices  $H(r, \lambda)$  and rotates locally about the

tangent  $\tau(r, \lambda)$  with a pitch almost equal to  $p$ ; hence, the  $H(r, \lambda)$  helices are deformed  $\chi$  cholesteric axes. In particular, the  $k=1/2$  disclinations of the  $DH^*$  derive from twisted  $\chi$  disclinations of the  $N^*$  phase, which pre-exist in the cybotactic group, where they have the same chirality as the  $N^*$  phase.<sup>8</sup>

### B. Twisted $\chi$ disclinations in a $N^*$ cybotactic group: Transverse screw dislocation densities

The *achiral* Sm-A DHs often stem at the  $N \rightarrow$  Sm-A transition from disclinations of strength  $k=1/2$  pre-existing in the  $N$  phase; see Sec. IV and Fig. 3. A similar process may take place in a Sm-A\*; a  $DH^*$  may stem from a  $\chi$  disclination  $L$  of strength  $k=1/2$ , but in a somewhat more subtle fashion. The mechanism proposed here applies directly to a type I transition; there are some complications for the type II transition, which we have not analyzed in detail (but see Sec. VII D).

We assume—in line with the conjecture made previously—that a  $\chi$  wedge disclination  $L$  sitting along a *straight* cholesteric axis takes a helical shape of pitch  $p$  such that the new disclination line (call it  $H$ ) now sits along a *twisted* cholesteric axis belonging to a cybotactic group. In this operation the rotation vector  $\Omega$  has been rotated toward the tangent  $\tau_H$  at any point of  $H$  and is now variable in direction. When eventually the transition to the Sm-A\* takes place,  $H$  transforms to a  $DH^*$  helical singularity, either by coupling with another line  $H'$  or by emitting  $DH^*$ s in the manner of Fig. 3. We analyze this process.

In the  $N^*$  phase a  $\chi$  disclination of strength  $k=m/2$ ,  $m \in \mathbb{Z}$  is equivalent to a dislocation of Burgers vector  $b=kp$ , and can take any shape as long as the rotation vector  $\Omega$  is *constant* in direction [6]. This flexibility can be expressed in terms of *dislocation densities* attached to the line  $L$ , with Burgers vectors  $\mathbf{b}_\perp$  orthogonal to  $\chi$ ; these  $\mathbf{b}_\perp$ 's are *continuous* translational symmetries of the  $N^*$  phase, so that the related dislocation densities can relax viscously to vanishing dislocation defects  $\delta\mathbf{b}_\perp \rightarrow 0$ . Thus, they do not bring any significant energy contribution to the line energy of  $L$ . We refer the interested reader to [15] for a thorough discussion of these points. The essential result to retain is that the flexibility of the disclination line is related to the viscous relaxation of symmetry-allowed continuous dislocations that are attached to the line.

$H$ , which is a disclination line with a *variable* rotation vector  $\Omega(P)$  along  $\tau_H(r, \lambda)$ , is different: its flexibility still requires the presence of attached defect densities, but these do *not* carry continuous symmetries of the  $N^*$  phase. Therefore, there is no possible viscous relaxation and the defect densities (*disclination densities* here) make a contribution to the line energy  $F_H$  of  $H$ . Again, we shall content ourselves with qualitative results; a detailed calculation of these continuous disclinations, based on the theory of Ref. [15], is given in Appendix B, as well as a discussion of the coupling of two  $H$  lines.

<sup>8</sup>The rotation vector  $\Omega$  of a  $\chi$  disclination is locally along the cholesteric axis  $\chi$  [6], here a twisted line.

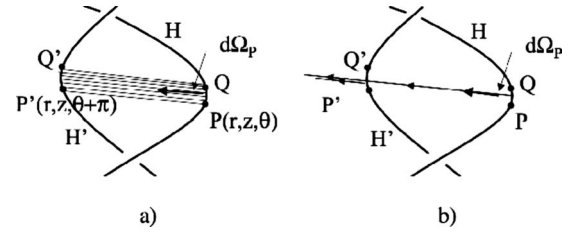


FIG. 7. (a) Disclination densities of rotation vectors  $d\Omega_p$  in the  $N^*$  phase, attached between  $P$  and  $Q=P+dP$  on  $H$ ,  $P'$ , and  $Q'=P'+dP$  on  $H'$ ; they form a stacking fault between  $H$  and  $H'$ . The helices  $H$  and  $H'$  are at the same constant distance  $\rho=r_H=r_{H'}$  of the central axis. The rotation vectors  $\Omega_p, \Omega_{p'}, \Omega_Q, \dots$  tangent to  $H$  and  $H'$  are not represented. (b) Cancellation outside the stacking fault of infinitesimal disclination lines attached to  $PQ$  and  $P'Q'$  at opposite points on  $H$  and  $H'$ ; these disclinations have the same orientation, but opposite rotation vectors.

Consider two lines  $H$  and  $H'$  with parallel axes of opposite rotations  $\Omega + \Omega' = 0$  or such that  $\Omega + \Omega'$  is a multiple of  $2\pi$ . They carry attached disclination densities of opposite signs which cancel outside the ribbon bordered by  $H$  and  $H'$ —the *stacking fault*—if the densities are conveniently coupled, as in Fig. 7. If  $\Omega = \Omega' = \pi$ , the pair  $H+H'$  is equivalent at a distance to a  $k=1$   $\chi$  disclination (equivalently a screw dislocation of Burgers vector  $b=p$ ). This result does not depend on the distance between  $H$  and  $H'$ ; therefore, a  $DH^*$  whose width is not ideal is feasible.

### C. Longitudinal screw dislocation densities

In Fig. 7, the disclination density is  $|d\Omega_p/(\rho^2 + \varpi^2)^{1/2}d\theta| = 2\rho/(\rho^2 + \varpi^2)$  (Appendix B) and reaches its maximum  $1/\rho$  for  $\rho = \varpi$ . This density vanishes in the Sm-A\* phase. Indeed,  $d\Omega_p$  is along the local director at the attachment of these densities along the  $k=1/2$  lines, and such a rotation is an allowed continuous symmetry in the Sm-A\* phase; the energy of the stacking fault proper can be viscously relaxed in the Sm-A\* phase.

An ideal  $DH^*$  is such that  $\rho = \varpi$ , precisely the value for which the disclination density—and thereby the stacking fault energy in the  $N^*$  cybotactic group—is the highest. Conversely, one expects that in the  $N^*$  phase the pair  $H+H'$  tends to be apart at a distance  $\rho < \varpi$  ( $\rho=0$  at equilibrium if the dominant term is the stacking fault energy; a complete solution would require solving the Ginzburg-Landau equations). The observed  $DH^*$ s are most often “thin,” indicating  $\rho < \varpi$ . This also manifests in DC not being fulfilled (see Fig. 5). The associated stresses can be relaxed by *edge dislocations* (cf. Sec. V).

In the  $N^*$  phase, the canceling out outside the stacking fault of the disclination densities  $d\Omega_p, d\Omega_{p'}$  requires  $r_H = r_{H'} = \rho/2$  ( $H, H'$  must have a common helical axis, the same pitch, and opposite strengths  $d\Omega_p + d\Omega_{p'} = 0$ ). If  $r_H \neq r_{H'}$ , either each of the two helices produces in the Sm-A\* phase single helical strands, of Burgers vectors  $p/2, p'/2$ , or both adjust their distances by emitting or absorbing *screw dislocations* in order to equalize their pitches to some value  $p''$ —in which case they eventually associate in a  $DH^*$  of

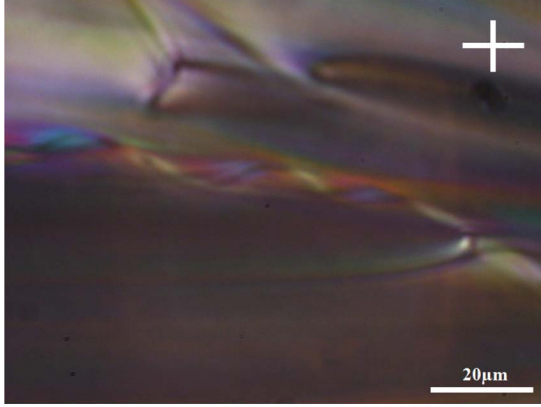


FIG. 8. (Color online) Helical ribbon associated with a parabolic FCD. Type II specimen, C9.

Burgers vector  $b=p''$ . Although  $p, p'$  are macroscopic, the differences  $p-p'', p'-p''$ , can be resolved into microscopic dislocation lines orthogonal to the layers either outside the  $DH^*$  cylinder or inside a ribbon (see below). The mechanism can be quite complicated, e.g., these dislocations can be attached by kinks to  $H$  and  $H'$ ; the  $H+H'$  complete coupling would then be effective only along the helical segments of the same level whose pitches are both equal to  $p''$ .

The edge and screw dislocations introduced in this paragraph are *quantized* symmetry-allowed dislocations. Thus, they cannot relax viscously, as continuous defects can.

Association of helical ribbons with other disclinations: We report on a quite frequent observation that might be related to a mechanism of production of screw dislocations as above. In Fig. 8, a long helical ribbon is interacting with a disclination belonging to a quasiparabolic FCD (PFCF): both constitutive conics have an eccentricity of  $\approx 1$ . The helical ribbon follows one of the parabolas, jumps over the region common to the two parabola apices (the helical defect is no longer fully visible), and then follows the other parabola.

This interaction explains if the ribbon is made of screw dislocations parallel on average to the helical axis. The stress field of the PFCF where the helical ribbon gathers is at the origin of the formation of the bundle: in effect the  $Sm-A^*$  layers are quasiorthogonal to the parabolic disclination in its vicinity, thereby orthogonal to the ribbon (a screw dislocation geometry), except in the region common to the two apices where precisely the ribbon is less visible; it is there certainly possible to parse it into its native dislocations. The interaction of screw dislocations all along FCD hyperbolas has already been documented (cf. [5], and references therein). The question of the helicity of screw dislocation bundles is new; it may be searched in the helical structure of the originative cybotactic group.

#### D. Comments on type II helical defect nucleation

A TGBA phase is made of a sequence of smectic slabs (thickness denoted  $\ell_b$ ) separated by twist grain boundaries (TGBs) that produce a rotation  $\alpha=\text{const}$  between two consecutive slabs [13]. The axis of rotation is parallel to the

smectic layers; the pitch along this axis is  $p=(2\pi/\alpha)\ell_b$ . The rotation angle is related to the screw dislocation content of the TGB; let  $\ell_d$  be the distance between dislocations in a slab,  $b=d_0$ , then  $2\sin(\alpha/2)=d_0/\ell_d$ .<sup>9</sup> The approximation  $\alpha \approx d_0/\ell_d$  is usually justified. Hence,

$$\varpi = \frac{p}{2\pi} = \frac{\ell_d \ell_b}{d_0}. \quad (15)$$

Let us assume that these microscopic dislocations in the  $Sm-A^*$  phase cover transversely and uniformly the ribbon which is bordered by  $H, H'$ , between which they are stretched. We show below—using the theory developed in [15], which yields Eq. (16)—that the maximum density of screw dislocations compatible with the size of their attachment to  $H, H'$  (this size is not vanishingly small) is  $2/d_0$  measured along these disclinations. But it happens that this is also the maximum value allowed by the density of TGB screw dislocations in the TGBA phase. The demonstration requires two assumptions: (1) that the pitch does not vary at the transition and (2) that  $r_H=r_{H'}=\varpi$ .<sup>10</sup> In all other cases ( $r_H \neq r_{H'}$ ) the density is smaller.

Because they proceed from TGBs formerly orthogonal to the  $DH^*$  axis, the number of dislocations is  $2\varpi/\ell_d$  per TGB area enclosed in the cylinder of radius  $\rho=\varpi$ . The slabs of thickness  $\ell_b$  are orthogonal to the  $\chi$  axis of the  $N^*$  phase, which as in Sec. VII B we suppose to be transformed to  $H$  and  $H'$ ; thus,  $2\varpi/(\ell_d \ell_b)=2/d_0$  per unit length of helical disclination. This is a maximum value of the screw dislocation density: the pitch has certainly increased at the transition, and a certain number of dislocations may have canceled by interacting with dislocations of opposite signs.

Each dislocation is attached to  $H, H'$  at kinks  $\vec{A}\vec{B}, \vec{A}'\vec{B}'$ . Consider the  $H$  kink  $\vec{A}\vec{B}=[u, v, w]$ ; it is such that [15]

$$2\sin\frac{\Omega}{2}\vec{\tau}_H \wedge \vec{A}\vec{B} = d_0[\alpha, \beta, \gamma], \quad (16)$$

where  $\vec{\tau}_H = \frac{1}{N}[-\varpi \sin \theta, \varpi \cos \theta, \varpi]$  is tangent to  $H$ ,  $[\alpha, \beta, \gamma]$  is a unit vector along the Burgers vector of the screw dislocation, and  $N = \sqrt{\rho^2 + \varpi^2} = \sqrt{2}\varpi$ . Without loss of generality, we assume that  $\theta=0, 2\pi, \dots$ ; then the Burgers vector is along the  $x$  axis,  $\alpha=1, \beta=\gamma=0$ . Hence, with  $\Omega=\pi$ , one gets  $\beta=\gamma=0 \rightarrow u=0, \alpha=1 \rightarrow \frac{2}{N}\varpi(w-v)=d_0$ . The kink  $\vec{A}\vec{B}$  is of extremal length when  $\vec{\tau}_H \cdot \vec{A}\vec{B} = \varpi(v+w)=0$ . Eventually,

$$u=0, \quad v = -\frac{d_0}{4\varpi}N = -\frac{d_0}{2\sqrt{2}}, \quad w = \frac{d_0}{4\varpi}N = \frac{d_0}{2\sqrt{2}}. \quad (17)$$

Such a dislocation is of screw character all along the straight segment that links two opposite kinks  $\vec{A}\vec{B}$  and  $\vec{A}'\vec{B}'$  at  $\theta$  and  $\theta'=\theta+\pi$ ; it is indeed normal to the layers since the layers are parallel, and since it is normal to one of them at  $r=0$ .

<sup>9</sup>The Burgers vector of the TGB screw dislocations is  $d_0$ , not  $2d_0$ , because the screw dislocations of the appropriate sign have a negative  $K_2$  contribution to the core energy; see Sec. VI A.

<sup>10</sup>We take  $r_H=r_{H'}=\varpi$  for simplicity. We know from Sec. VII C that any deviation to this condition can be plastically relaxed by edge dislocations.

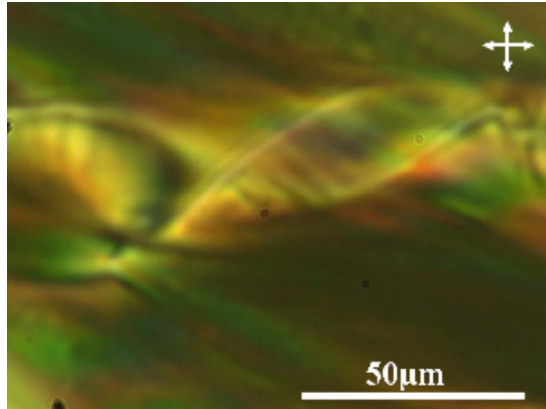


FIG. 9. (Color online) Helical ribbon in cholesteryl nonanoate (C9) with its axis parallel to the polarizer. The dark background indicates that outside the helical ribbon the smectic layers are perpendicular to the axis of the helical ribbon.

Notice that the length of the kink is  $|\vec{AB}| = |\vec{A'B'}| = d_0/2$ , which is the minimal expected value if *all* the screw dislocations of the TGBs are preserved at the transition from the TGBA phase to the Sm- $A^*$  phase.

There are thus two extreme situations resulting from the presence of the TGB screw dislocations in the DH\*s of the Sm- $A^*$  phase. In a first case these dislocations cover a twisted uniform ribbon bordered by the disclinations  $H$  and  $H'$ . In a second case the dislocations are far from their maximum allowed density and then gather into bundles between which the DH\* recovers a geometry comparable to an ideal DH. This is observed in Fig. 9, which illustrates the type II C9 phase. Figure 10 shows a quite similar observation, but made in C14, which is type I; this might be illustrative of case (ii) in Sec. VI C.

### VIII. CONCLUSION

This paper contains two parts that are quite distinct:

(i) The first one is an extended review of the notion of double helical defect in Sm- $A$  compounds, with stress put on the concept of isometry [parallelism of the layers—in that sense DHs belong to the same family as focal conic domains (FCDs), except that the locus of the centers of curvature of

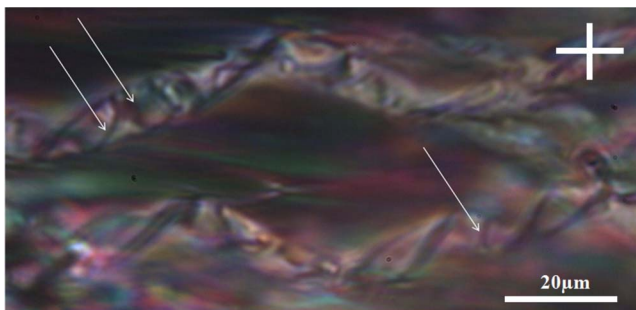


FIG. 10. (Color online) Probable screw dislocation bundles (shown by arrows) linking two helical disclinations observed in C14.

the parallel surfaces is made of two surfaces, not two conics]. Isometry relates to the Darboux condition, the application of a theorem of surface geometry theory which gives clues for deciding through mere optical observation that the layers are parallel.

(ii) The second one is a detailed investigation of the parent defects DH\*s in Sm- $A^*$  compounds, i.e., thermodynamical phases with chiral molecules orthogonal to a family of layers. We compare them fully with DHs—at experimental and theoretical levels; a key feature is that isometry is no longer satisfied—and also between them according to the nature of the transition, depending on whether it is type I ( $N^* \rightarrow \text{Sm-}A^*$ ) or type II ( $N^* \rightarrow \text{TGBA} \rightarrow \text{Sm-}A^*$ )—at a theoretical level.

Although there are no topological obstructions to finding with Sm- $A^*$ s the exact analogs of DHs, and although in light microscopy investigations DH\*s look at first sight much similar to DHs—in both cases one observes two coupled helical defects—the differences are considerable. They originate from the generation process of these DH\*s in the  $N^*$  phase. It is indeed our conjecture that the geometry of DH\*s reproduces the topology of cybotactic groups of the  $N^*$  phase, which for that purpose are studied from a geometric point of view.

Another element central in our investigation is the difference in free energy of screw dislocations of opposite chiralities. The preferred chirality is the same as that of the  $N^*$  phase; this is also the chirality of the cybotactic group, thereby the preferred chirality of the DH\*s. This result appears as a clear experimental result.

Whereas the theoretically foreseen differences between types I and II DH\*s are not easily empirically reachable, the DH\*s exhibit a number of common characters, which enter their theoretical description and differentiate them from DHs. Among them is the fact that the Darboux condition and the Kirchhoff relation at nodes are not satisfied. Furthermore, DH\*s most generally form ribbons, bordered by the helical defects, and covered with screw dislocations of microscopic Burgers vectors either uniformly—these dislocations can be transverse to the ribbon or longitudinal—or forming bundles of screw dislocation segments attached to the helical defects. The present state of the analysis suggests that the theory should be extended by taking into account the fluctuations, at least in mean-field theory, and the experiments completed with freeze-fracture microscopy investigations.

### ACKNOWLEDGMENTS

We thank Pr. J. Friedel for suggesting the consideration of the concept of stacking fault in the  $N^*$  phase. We are grateful to a referee for extremely valuable comments on the twist carried by a double Burgers vector screw dislocation and to Pr. J. M. Robbins for discussions. This is IGP contribution no. 3056 (M.K.).

### APPENDIX A: NYE'S DISLOCATION DENSITIES

The density tensor of a discrete dislocation  $L$  of Burgers vector  $b_i, i=1, 2, 3$  can be written as

$$\alpha_{ij} = \delta_j(L)b_i.$$

This quantity measures the *plastic* strains [16];  $\alpha_{ij}$  can be also expressed in terms of the contortion tensor  $K_{ij}$ , which measures the associated plastic rotations [17]:

$$\alpha_{ij} = \delta_{ij}K - K_{ji}, \quad K = K_{11} + K_{22} + K_{33}.$$

This expression is valid insofar as the strains  $e_{ij}$  vanish identically, a condition that can be achieved in a liquid crystal. It is indeed the condition of isometry in a layered or columnar liquid crystal phase.

One can show [8] that for any unit vector that has constant coordinates in the rotating frame (the normal  $\mathbf{n}$  to the layers is such a vector), one has

$$\mathbf{n} \cdot \text{curl } \mathbf{n} = \sum_{ij} K_{ij}n_i n_j - K.$$

For a screw dislocation the only nonvanishing component of the dislocation density tensor is  $\alpha_{33} = \delta_3(L)b_3$ . Hence, after a simple calculation, one gets, with  $n_i = \pm \delta_{i3}$ ,  $b_i = b\delta_{i3}$ ,

$$\mathbf{n} \cdot \text{curl } \mathbf{n} = -2K = -b\delta_3(L).$$

Here,  $L$  is along the  $\hat{z}$  axis. The use of the dislocation density tensor and of the contortion tensor for a *discrete* defect is inspired by the approach of Kröner [16] and Nye [17] for *continuous* defects. The present result is obtained under the assumption that  $b$  is small.

A less general demonstration, but of a simple physical content, is as follows. Consider a planar twist grain boundary made of parallel equidistant screw lines  $L_j$ , repeat distance  $\ell$ , and Burgers vector  $b$ . This plane separates two smectic grains, misoriented one with respect to the other by the angle  $\omega \approx |b|/\ell$  [15], assuming  $\omega$  is small. We can write  $\omega = \int |\mathbf{n} \cdot \text{curl } \mathbf{n}| dx$  ( $\hat{x}$  orthogonal to the twist boundary is the axis of twist). Since  $\omega \approx |b|/\ell$  also reads  $\omega \approx |b|/\ell \int \delta(x) dx$ , we have  $|\mathbf{n} \cdot \text{curl } \mathbf{n}| = (|b|/\ell) \delta(x)$ .  $1/\ell$  is the density of dislocations, which is also the mean value of the comb periodic function  $\sum_{j=-\infty}^{\infty} \delta(y - y_j)$ , with  $y_j = j\ell$  ( $\hat{y}$  is orthogonal to the dislocations in the twist boundary). Hence, assuming that  $|\mathbf{n} \cdot \text{curl } \mathbf{n}|$  is the mean value of the distribution  $\sum_j |\mathbf{n} \cdot \text{curl } \mathbf{n}|_j$ , each  $|\mathbf{n} \cdot \text{curl } \mathbf{n}|_j$  assigned to a dislocation  $L_j$ , one gets by identification

$$|\mathbf{n} \cdot \text{curl } \mathbf{n}|_j = |b| \delta(x) \delta(y - y_j) = |b| \delta_3(L_j).$$

Hence, each dislocation  $L_j$  carries a rotation rate  $|\mathbf{n} \cdot \text{curl } \mathbf{n}|_j$  obeying the expression derived above in a more general context.

We have not yet made reference to the fact that  $\mathbf{n} \cdot \text{curl } \mathbf{n}$  is a pseudoscalar. We assume, as it is usually done, that the frame of reference is right handed. In such a frame a right-handed cholesteric  $N^*$  has a positive pitch  $p = \frac{2\pi}{q}$ . In its ground state  $\mathbf{n} \cdot \text{curl } \mathbf{n} = -q < 0$ , according to Eq. (4). By analogy, the above relation  $\mathbf{n} \cdot \text{curl } \mathbf{n} = -b\delta_3(L)$  implies that for  $b > 0$  the layers surrounding the screw dislocation have the configuration of a right-handed helix. This fixes the convention on the sign of  $b$ .

## APPENDIX B: CONTINUOUS DISCLINATIONS AT THE $N^* \rightarrow \text{Sm-A}^*$ transition

The coordinates of a helix  $H$  of radius  $r_H$  can be written as

$$H \equiv \{r_H \cos \theta, r_H \sin \theta, \varpi \theta\},$$

with an evident notation  $\varpi = p/2\pi$ . We assume in this appendix that  $H$  is a  $\chi$  axis of a distorted cholesteric, and that there is a  $\chi$  disclination of strength  $k=1/2$  along  $H$ . Let  $\boldsymbol{\tau}_H$  be the unit tangent at a point on  $H$ ; the rotation vector of the disclination line is

$$\boldsymbol{\Omega}_H = 2 \sin \frac{\Omega}{2} \boldsymbol{\tau}_H \propto \{-r_H \sin \theta, r_H \cos \theta, \varpi\}, \quad \Omega = \pi.$$

The curvature of  $H$  requires between two infinitesimally close points  $P$  and  $Q = P + \boldsymbol{\tau}_H(P)ds$  on  $H$  the attachment of a density of line defects. Let  $M$  be a running point on the cut surface  $\sigma$  of  $H$ . The variation of the relative displacement of the two lips of  $\sigma$  between  $P$  and  $Q$  is [15]

$$\boldsymbol{\delta} = 2 \sin \frac{\Omega}{2} [\boldsymbol{\tau}_H(Q)Q\vec{M} - \boldsymbol{\tau}_H(P)P\vec{M}],$$

which can also be written as

$$\boldsymbol{\delta} = 2 \sin \frac{\Omega}{2} d\boldsymbol{\tau}_H \times P\vec{M} + \mathcal{O}(2).$$

Neglecting second-order terms, it remains an *infinitesimal disclination* whose rotation vector is

$$d\boldsymbol{\Omega}_H = 2 \sin \frac{\Omega}{2} d\boldsymbol{\tau}_H \propto \{-\cos \theta, \sin \theta, 0\} d\theta,$$

where  $d\boldsymbol{\Omega}_H$  is not a rotation of symmetry of the  $N^*$  phase. Therefore, the infinitesimal disclinations attached to  $H$  do not relax viscously and form a *stacking fault*  $H$  whose energy adds to the free energy of the line  $H$  proper. At this stage, it simplifies the analysis to take the local director  $\mathbf{n}$  along  $d\boldsymbol{\Omega}_H$ ;  $\mathbf{n}$  belongs to the local cholesteric plane orthogonal to  $\boldsymbol{\tau}_H$ .

The energy is bounded if the line  $H$  is paired with a line  $H'$  of opposite rotation vectors at corresponding points, or such that  $\Omega + \Omega'$  is a multiple of  $2\pi$ . The example of interest for us is when  $\Omega = \Omega' = \pi$ , with two helical  $k=1/2$  wedge disclination lines at the same distance  $\rho = r_H = r_{H'}$  of the axis of the helices, displaced one with respect to the other by a translation  $p/2$  along this axis. Two points  $P$  (on  $H$ ) and  $P'$  (on  $H'$ ) can be paired in such a way that  $\vec{OP} = -\vec{OP}' = \rho\{\cos \theta, \sin \theta, 0\}$ , with

$$\boldsymbol{\Omega}(P) = 2\{-\rho \sin \theta, \rho \cos \theta, \varpi\}/N,$$

$$\boldsymbol{\Omega}(P') = 2\{\rho \sin \theta, -\rho \cos \theta, \varpi\}/N,$$

where  $N^2 = \rho^2 + \varpi^2$ . The corresponding infinitesimal rotation vectors in  $P$  and  $P'$  are

$$d\boldsymbol{\Omega}(P) = -2\rho\{\cos \theta, \sin \theta, 0\}d\theta/N,$$

$$d\boldsymbol{\Omega}(P') = 2\rho\{\cos \theta, \sin \theta, 0\}d\theta/N.$$

They are opposite and relate to disclination lines of opposite

orientations, which can be moved at will, provided that they remain attached at  $P$  and  $P'$ , and that  $d\mathbf{\Omega}(P)$  and  $d\mathbf{\Omega}(P')$  are constant vectors. Adding up the two disclinations along the same line, it remains a disclination segment  $P\vec{P}'$ , oriented from  $P$  to  $P'$ , attached to  $H$  and  $H'$ , with a rotation vector

density equal to  $d\mathbf{\Omega}_p$  (Fig. 7).

The pair  $H+H'$  is therefore equivalent at a distance to a  $\chi$  disclination of strength  $k=1$  or, equivalently, a screw dislocation of Burgers vector  $b=p$ . This result does not depend on the radius  $\rho$ .

- 
- [1] C. Meyer, H. Logbo, B. Briouel, J.-C. Picot, Y. Nastishin, and M. Kleman, *Liq. Cryst.* **37**, 1047 (2010).
- [2] C. E. Williams, *Philos. Mag.* **32**, 313 (1975).
- [3] M.-F. Achard, M. Kleman, Y. A. Nastishin, and H. T. Nguyen, *Eur. Phys. J. E* **16**, 37 (2005).
- [4] M. Kleman and O. D. Lavrentovich, *Liq. Cryst.* **36**, 1085 (2009).
- [5] M. Kleman, C. Meyer, and Y. A. Nastishin, *Philos. Mag.* **86**, 4439 (2006).
- [6] M. Kleman, O. D. Lavrentovich, and Y. A. Nastishin, in *Dislocations and Disclinations in Mesomorphic Phases*, edited by F. R. N. Nabarro and J. P. Hirth, *Dislocations in Solids* Vol. 12 (Elsevier, Amsterdam, 2004), Chap. 66, p. 147.
- [7] F. Livolant and Y. Bouligand, *Chromosoma* **80**, 97 (1980).
- [8] M. Kleman, *Points, Lines and Walls* (Wiley, Chichester, England, 1982).
- [9] M. Baron *et al.*, *Pure Appl. Chem.* **73**, 845 (2001).
- [10] S. Garoff and R. B. Meyer, *Phys. Rev. Lett.* **39**, 225 (1977).
- [11] G. Darboux, *Leçons sur la Théorie Générale des Surfaces* (Gauthier-Villars, Paris, 1894).
- [12] P.-G. de Gennes and J. Prost, *The Physics of Liquid Crystals*, 2nd ed. (Clarendon, Oxford, 1995).
- [13] S. R. Renn and T. C. Lubensky, *Phys. Rev. A* **38**, 2132 (1988).
- [14] T. C. Lubensky, *J. Phys. Colloq.* **C1-36**, 151 (1975).
- [15] M. Kleman and J. Friedel, *Rev. Mod. Phys.* **80**, 61 (2008).
- [16] E. Kröner, in *Physics of Defects*, edited by R. Balian, M. Kleman, and J.-P. Poirier, *Les Houches Session XXXV* (North-Holland, Amsterdam, 1981), Chap. 3, p. 215.
- [17] J. F. Nye, *Acta Metall.* **1**, 153 (1953).